

Statistics of Strange Attractors by Generalized Cell Mapping

C. S. Hsu¹ and Myun C. Kim¹

Received November 10, 1983; revised May 16, 1984; July 20, 1984

It is proposed in this paper to use the generalized cell mapping to locate strange attractors of dynamical systems and to determine their statistical properties. The cell-to-cell mapping method is based upon the idea of replacing the state space continuum by a large collection of state space cells and of expressing the evolution of the dynamical system in terms of a cell-to-cell mapping. This leads to a Markov chain which in turn allows us to compute all the statistical properties as well as the invariant distribution. After a general discussion, the method is applied in this paper to strange attractors of a variety of systems governed either by point mappings or by differential equations. The results indicate that it is a viable, effective and attractive method. Some comments on this method in comparison with the method of direct iteration will also be made.

KEY WORDS: Strange attractors; statistical properties of strange attractors; invariant distribution; cell-to-cell mapping; generalized cell mapping; nonlinear dynamical systems; Hénon–Pomeau map; Zaslavskii map; forced Duffing systems.

1. INTRODUCTION

In recent years the phenomenon of strange attractors has received a great deal of attention in the field of nonlinear dynamics and dynamical systems. The literature is too vast to be quoted extensively here; many of the papers may be found referred to in Refs. 1–5. The basic intrigue of this phenomenon comes from the observation that while a strange attractor yields a chaotic motion, the originating system could very well be entirely deterministic in nature. Not only is the phenomenon interesting physically and

¹ Department of Mechanical Engineering, University of California, Berkeley, California 94720.

mathematically, but it also appears in many different fields. Therefore, it deserves to be studied in great depth.

In an unrelated direction, a method of cell-to-cell mapping for nonlinear system analysis has been introduced in the last few years.⁽⁶⁻¹²⁾ Preliminary studies show that the method has a great potential as a tool for studying the global properties of nonlinear systems. The basic idea of cell-to-cell mapping is to consider the state space of a dynamical system not as a continuum but as a large collection of state cells and to express the behavior of the system in terms of an evolution process of cell-to-cell mapping. Two kinds of cell mappings have been introduced and are being developed. The first kind has been called "Simple Cell Mapping" (SCM) in which a cell is allowed to have only one single mapping image. The second kind called "generalized cell mapping" (GCM) is a mapping where a cell under the mapping can have several image cells with a certain probability for each image cell. When a dynamical system is described in terms of a GCM, it leads naturally to a stationary Markov chain and the transition probability matrix determines completely the behavior of the system. Generalized cell mapping is discussed in Refs. 8 and 9. The method uses the theory of Markov chains extensively. Well-known books on that topic are Refs. 13-15.

In this paper we link the topic of strange attractors to the topic of GCM by using the concepts and techniques of GCM to find the location, invariant distribution, and statistical properties of a strange attractor. First, in Section 2 we discuss the minimum cell set which covers a strange attractor. We then show in Section 3 how strange attractors can be linked very naturally to GCM. In the context of GCM a strange attractor will appear as an acyclic persistent group of a Markov chain. A strange attractor consisting of K separate pieces will appear as a persistent group of period K . We shall also discuss in Section 3 how to actually find the persistent group which will represent a strange attractor and to determine its transition probability. Having the transition probability matrix of the Markov chain on hand, one can then easily calculate the invariant distribution and hence study the statistical properties of the strange attractor, such as the mean values, variances, standard deviations, moments of various orders, and correlation functions. This will be discussed in Section 4. We hope that the analysis given in Sections 3 and 4 will clearly demonstrate that the method of GCM is indeed a very natural tool to use when studying strange attractors.

The purpose of the paper is to discuss the methodology of using GCM to study the statistical properties of strange attractors. However, in order to assess the viability and efficacy of the method, we also apply it to several specific problems in Sections 5 and 7-9. Some of the strange attractors are well known. Others are strange attractors whose existence or statistical properties have not been studied before. We shall mostly be concerned with

strange attractors of point mappings. In Section 9 we shall however study a strange attractor which is originated from a dynamical system governed by a differential equation.

With regard to the Zaslavskii map studied in Section 8, we wish to cite here the work by Jensen and Oberman⁽⁵⁾ in which a detailed and excellent study of statistical properties of strange attractors of Zaslavskii map is made by using a path integral method. In relation to Ref. 5, the present paper might be said to be more computationally oriented.

In Section 6 we make some comments about the present method in comparison with the direct method of iteration. Besides comparing the computation effort required, we also point out the basic conceptual difference between the two approaches.

With regard to partitioning a state space, the idea dates back, at least, to Kolmogorov, Tihomirov, and Sinai, connected with their study of system entropy; see, for instance, Refs. 16–18. The present method is based upon the same idea of partitioning the state space into cells. However, being a more computation-oriented rather than analysis-oriented method, its development follows a somewhat different line. With regard to the idea of using cells, the reader may also wish to refer to a very instructive paper by Shaw⁽¹⁹⁾ in which the notion of cells of a minimum but finite size is also discussed.

2. COVERING SETS OF CELLS FOR STRANGE ATTRACTORS

Consider an N -dimensional point mapping

$$\mathbf{x}(n + 1) = \mathbf{G}(\mathbf{x}(n)) \tag{2.1}$$

where $\mathbf{x}(n)$ is an N vector. When a strange attractor exists for a point mapping, the sequence of the mapping points $\mathbf{x}(n)$ for sufficiently large n and beyond covers and stays in a specific domain of the state space without ever repeating itself. The precise coverage of strange attractors is only known for a very few cases. Also, for most strange attractors there seems to exist a cascade of finer and finer structure within the attractor. While this is the most intriguing feature of the strange attractors, because of the never-ending nature of the cascade it does not seem to be practical to determine the coverage and the structure exactly and explicitly in all the detail.

As stated earlier, the basic idea of GCM is to divide the state space into a collection of a large number of cells. Let us assume that a cell state space has been set up. When referred to a cellularly structured state space, a strange attractor will reside inside a set of cells. We shall call this set the *covering* set of the strange attractor and denote it by D_{SA} . It is always a finite set. In principle, it is a relatively simple matter to determine precisely

all the member cells of D_{SA} by iterating the map with a sufficiently large number of times. However, in practice, the number of iterations required could be very large. For instance, for the well-known Hénon–Pomeau map with $a = 1.4$ and $b = 0.3$ and using a cell size 0.01×0.00333 , even after iterating 30-million times, one or two straggler members cells are still being discovered after every million iterations. Thus, other methods of generating strange attractors are desirable.

3. PERSISTENT GROUPS REPRESENTING STRANGE ATTRACTORS

A persistent group of a stationary Markov chain^(13–15) of a GCM^(8,9) has the property that each cell in the group communicates with every other cell of the group. This is also the property of the covering set of cells of a strange attractor. Thus, in the context of GCM a strange attractor can be expected to show up as a persistent group. A one-piece strange attractor will show up as an acyclic persistent group and a K -piece strange attractor will in general show up as a persistent group of period K . For this reason one could expect that it would be possible to use GCM to generate a cell set B_{SA} which represents the strange attractor in question. We now describe how this can be done in principle and how to do this in a practical way.

3.1. Basic Idea of Generating the Cell Set B_{SA}

Let cells be denoted by integer-valued N -vectors \mathbf{Z} . Under mapping (2.1), a cell \mathbf{Z} can have a number of image cells.⁽⁸⁾ Let this number be denoted by $I(\mathbf{Z})$. Let the i th image cell of \mathbf{Z} be denoted by $\mathbf{C}_{(i)}(\mathbf{Z})$ and the complete set of the image cells of \mathbf{Z} be denoted by $A(\mathbf{Z})$. The probability of cell \mathbf{Z} being mapped into an image cell \mathbf{Z}' will be denoted by $p_{\mathbf{Z}'\mathbf{Z}}$ where $\mathbf{Z}' \in A(\mathbf{Z})$. We have, of course,

$$\sum_{\mathbf{Z}' \in A(\mathbf{Z})} p_{\mathbf{Z}'\mathbf{Z}} = 1 \quad (3.1)$$

A set of cells representing the strange attractor can be generated in the following manner. Let cell $\mathbf{Z}_{(1)}$ be a cell in the set D_{SA} . (On this aspect of how to start the procedure, a discussion will be given in Section 3.5.) An array M_{SA} is set up to include the discovered member cells of B_{SA} . Obviously, $\mathbf{Z}_{(1)}$ will be the first member of this array. Having $\mathbf{Z}_{(1)}$, one can find all the $I(\mathbf{Z}_{(1)})$ number of image cells of $\mathbf{Z}_{(1)}$ and the associated probabilities. One of the image cells of $\mathbf{Z}_{(1)}$ could be $\mathbf{Z}_{(1)}$ itself. Others, if $I(\mathbf{Z}_{(1)}) > 1$, will be newly discovered cells of B_{SA} . Let the number of new cells be m_1 . These m_1 new cells will then be entered into the array M_{SA} which has now $1 + m_1$ members.

Next, we take the second member of M_{SA} , say, $Z_{(2)}$, and find its image cells. Let m_2 of these image cells are not in M_{SA} . These will then be added to the array M_{SA} which has now $1 + m_1 + m_2$ members. Next, we take the third member $Z_{(3)}$ of M_{SA} , find its image cells, and update the array M_{SA} . This process is continued until the image cells of the last member of the current set M_{SA} are all found to be already in M_{SA} and, therefore, no more updating of M_{SA} will be needed. This set M_{SA} is now closed and it is then the set B_{SA} we are seeking. For convenience we denote the number of members in B_{SA} by $N(B_{SA})$.

3.2. Limiting Probability of B_{SA} and Invariant Distribution

Having determined the membership of B_{SA} and along the way also obtained $p_{Z'Z}$, $Z \in B_{SA}$, $Z' \in A(Z)$, we have on hand the transition probability matrix \mathbf{P} of a Markov chain whose components p_{ij} , $i, j = 1, 2, \dots, N(B_{SA})$, denote the transition probability from cell j to cell i . It is then a straightforward matter to determine the limiting probability vector \mathbf{p} of this persistent group with components p_i , $i = 1, 2, \dots, N(B_{SA})$. A very practical method of finding this limiting probability vector \mathbf{p} is simply the power method (also known as the iteration method) which utilizes the fact that \mathbf{p} is merely the eigenvector of \mathbf{P} corresponding to the dominant eigenvalue 1. A simple interpretation of this limiting probability vector is that on the long-term basis the chance of the mapping process to land in cell $Z_{(i)}$ is p_i .

This limiting probability vector is, of course, nothing but a discrete version of the invariant distribution of the strange attractor.^(1,19) Thus, by using this method of GCM, the invariant distribution can be readily computed once the transition probability matrix is known, without the need of resorting to special methods, such as the Fokker–Planck equation and so forth.

3.3. The Periodicity of B_{SA}

The persistent group may be an acyclic group or a periodic group, depending upon whether the period of B_{SA} is 1 or >1 . There are different ways of determining this particular property of a persistent group. The simplest is again the power method. Starting with an initial probability distribution $\mathbf{P}_{(0)} = (1, 0, 0, \dots, 0)^T$ and iterating a large number of times, if the probability distribution from step to step iteration shows a pattern of subgroup to subgroup migration, then B_{SA} is a periodic persistent group of period larger than 1. Otherwise, it is an acyclic persistent group. Once the group is known to have a period larger than 1, its precise period and the limiting probability distribution within each subgroup can then be readily

determined. If B_{SA} is a persistent group of period K , then the strange attractor is a periodic attractor of period K or higher and is consisted of K or more separate pieces in the state space.

3.4. Comparison of D_{SA} and B_{SA}

For a given cellularly structured state space there are D_{SA} which is the minimum set of cells in which the strange attractor lies and B_{SA} which also covers the strange attractor but is obtained by using the GCM method. In general, we cannot expect these two sets to be the same. Because of discretization of the state space, the method of GCM could bring into B_{SA} extraneous cells which are not elements of D_{SA} . However, D_{SA} is contained in B_{SA} . Moreover, we note that the extraneous cells will have extremely small limiting probabilities and, therefore, their presence in B_{SA} will have a negligible effect on the computed statistical properties of the strange attractor by using B_{SA} .

3.5. The Starting Cell of the Procedure

Here we make some comments on the selection of the starting cell for the generating process. In many cases the strange attractor results from a cascade of bifurcation. At each stage of bifurcation, as a system parameter is increased or decreased, a certain periodic solution becomes locally unstable and new solutions of higher period come into being. In such instances there are points, infinitely near these unstable periodic points, which are in the strange attractor. Thus, a cell containing one of these unstable periodic points can be used as the starting cell for the process described in Section 3.1 to generate the persistent group. In any event, it is a simple matter to incorporate a step in the generating process to test whether the starting cell does communicate with other cells of the group and, therefore, is indeed a member of a persistent group.

3.6. Sampling Method for Implementation

In Section 3.1 we have explained how the GCM method can be used to find, in principle, the set B_{SA} . The method, however, requires finding all the image cells of a cell and the associated probability distribution. In general, this is a very difficult task for nonlinear mappings. Thus, as a practical matter, we need a viable method of implementation. Up to now we find the straightforward sampling technique to be a very effective one. For each cell, say, cell Z , we simply divide it into M subcells of equal size and compute the mapping images of the M center points of these subcells according to (2.1).

If M_1 image points lie in cell Z_1 , M_2 points lie in cell Z_2, \dots , and M_m points in cell Z_m , then we assign

$$I(\mathbf{Z}) = m, \quad C_{(i)}(\mathbf{Z}) = Z_i, \quad p_{Z_i, \mathbf{Z}} = M_i/M, \quad i = 1, 2, \dots, I(\mathbf{Z}) \quad (3.2)$$

This is an extremely simple and effective method, applicable for any nonlinearity and can be used for point mappings of any dimension.

4. STATISTICAL PROPERTIES OF STRANGE ATTRACTORS

Most of the recent studies of strange attractors of specific point mappings involve repeated mapping to generate a large number of mapping points in order to demonstrate the existence of the strange attractor and to exhibit any fine structure which may exist within the attractor. While determining the location of the strange attractor should be the first order of business, we are also interested in the strange attractor as a possible *long-term response* of the dynamical system. Since the response is chaotic it is natural to study the response properties in a statistical sense. To determine the statistical properties numerically one can use the straightforward method of repeated mapping. These statistical properties represent the time averages. This approach, while practical, is perhaps not particularly attractive because a very large number of iterations is usually required owing to the standard error of order $N^{-1/2}$ associated with the process, N here being the sample size.

Here we describe an alternative way via the GCM method which seeks the statistical properties of a strange attractor through spatial averages over the state space. Using the generating process of Section 3.1 we can find B_{SA} and the associated transition probability matrix. This transition matrix determines completely the behavior of the persistent group and, hence, approximately the behavior of the strange attractor. We can expect that the accuracy of approximation will be improved if we use smaller cell sizes. In fact, the examples to be shown later indicate that with a reasonably small cell size the accuracy of approximation on the statistical properties is already quite satisfactory.

Maximum and Minimum Excursions. First, having determined B_{SA} , we can easily find the maximum and minimum excursions of the persistent group in each dimension of the state space.

Mean Value μ . Let $x_{(k)}$ be the position vector of the center point of

cell $\mathbf{Z}_{(k)}$. Within the accuracy of discretization of the state space into cells, the mean value vector of the response is then given by

$$\boldsymbol{\mu} = \sum_{k=1}^{N(B_{SA})} \mathbf{x}_{(k)} p_k \tag{4.1}$$

where p_k is the limiting probability of cell $\mathbf{Z}_{(k)}$.

Central Moments $\bar{m}_{\alpha_1 \alpha_2 \dots \alpha_N}$. The central moments are given by

$$\bar{m}_{\alpha_1 \alpha_2 \dots \alpha_N} = \sum_{k=1}^{N(B_{SA})} \prod_{j=1}^N (x_{j(k)} - \mu_j)^{\alpha_j} p_k \tag{4.2}$$

where $x_{j(k)}$ is the j th component of $\mathbf{x}_{(k)}$ and μ_j is the j th component of $\boldsymbol{\mu}$.

Central Correlation Function Matrix $\bar{\mathbf{R}}(\mathbf{k})$. Let $\bar{\mathbf{R}}(k)$ be the central correlation function matrix between $(\mathbf{x}(n) - \boldsymbol{\mu})$ and $(\mathbf{x}(n+k) - \boldsymbol{\mu})$ and $\bar{R}_{ij}(k)$ be its (i, j) th component, representing the central correlation between $x_j(n)$ and $x_i(n+k)$. Then we have

$$\bar{R}_{ij}(k) = \sum_{l=1}^{N(B_{SA})} \sum_{m=1}^{N(B_{SA})} (x_{i(l)} - \mu_i) p_{lm}^{(k)} p_m (x_{j(m)} - \mu_j) \tag{4.3}$$

where $p_{lm}^{(k)}$ is the (l, m) th component of \mathbf{P}^k , the k th power of the transition probability matrix \mathbf{P} .

This completes the general discussion on using the GCM method to obtain statistical information of a strange attractor. In the next few sections we apply the general discussion to various specific problems.

5. A STRETCH–CONTRACTION–REPOSITION MAP

We first consider a very simple “stretch–contraction–reposition” map⁽⁴⁾ which maps a unit square onto itself:

$$\begin{aligned} x_2(n+1) &= \lambda_1 x_2(n) \pmod{1} \\ x_1(n+1) &= \lambda_2 x_1(n) + x_2(n) - \lambda_1^{-1} x_2(n+1) \end{aligned} \tag{5.1}$$

where λ_1 is to be a positive integer and λ_2 a positive number less than 1. This map has a strange attractor for certain values of λ_1 and λ_2 . In this section we use the GCM method to locate the strange attractor and to determine its statistical properties.

Let the state space of the unit square be divided into $N_1 \times N_2$ cells where N_1 and N_2 are the numbers of intervals in the x_1 and x_2 directions. We shall present here only the results for the case $\lambda_1 = 3$ and $\lambda_2 = 1/4$. The

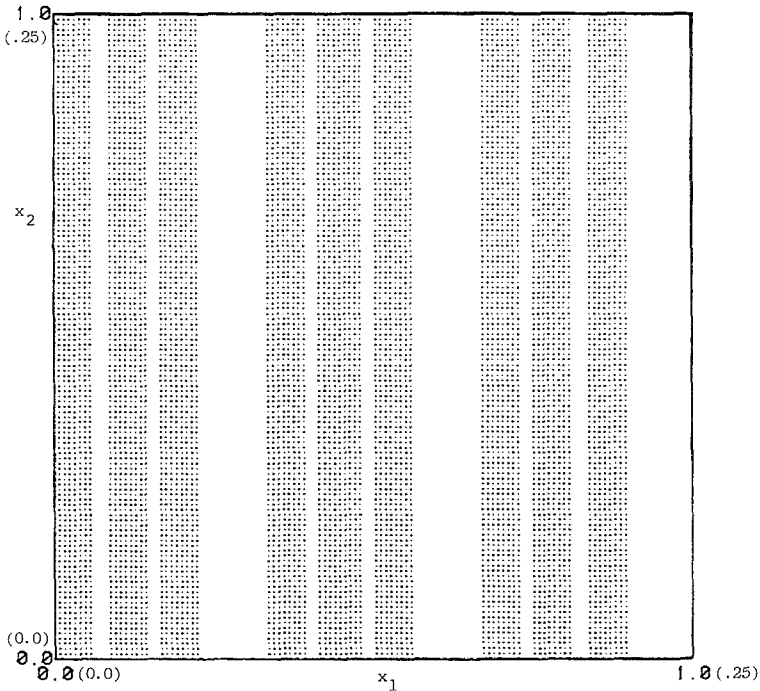


Fig. 1. The persistent group representing the strange attractor of map (5.1) for $\lambda_1 = 3$ and $\lambda_2 = 1/4$. $N_1 = N_2 = 125$. Also representing $1/16$ of the persistent group covering the lower left corner of the unit square for $N_1 = N_2 = 500$.

number of sampling points used within each cell is 5×5 . (See the discussion given in Section 3.6.) Figure 1 gives the set B_{SA} for $N_1 = N_2 = 125$. Each point in the figure represents a member cell of B_{SA} . The figure clearly shows the tripartition of the unit square and the further tripartition within each one-third of the square. If we use $N_1 = N_2 = 500$, we can disclose a much finer structure of the strange attractor in the form of a further tripartitioning of the covering set. In fact, when we relabel Fig. 1 with the abscissa covering $0 \leq x_1 < 1/4$ and the ordinate covering $0 \leq x_2 < 1/4$ such as shown by the numbers in parentheses, then that figure also gives exactly the set B_{SA} of the strange attractor for the lower-left corner of the unit square covering an area equal to $1/16$. This clearly demonstrates the scale invariant character of the structure of this strange attractor.

Next, we examine the statistical properties of the strange attractor. It turns out that because of the especially simple nature of the mapping the statistical properties can be evaluated analytically and exactly. Let

$$E_{(l)}^{(k)} = \binom{k}{l} \frac{\lambda_2^l}{\lambda_1^{k-l+1}} \sum_{j=1}^{\lambda_1} (j-1)^{k-l} \tag{5.2}$$

Then the moments $m_{\alpha_1,0}$, $\alpha_1 \geq 1$, are given by

$$m_{\alpha_1,0} = \left[\sum_{l=0}^{\alpha_1-1} E_{(l)}^{(\alpha_1)} m_{l,0} \right] / [1 - E_{(\alpha_1)}^{(\alpha_1)}] \quad (5.3)$$

where the moments m_{α_1,α_2} are defined by a formula similar to (4.2). The moment $m_{0,0}$ is logically taken to be 1. Similarly, we find

$$m_{0,\alpha_2} = \frac{1}{\alpha_2 + 1} \quad (5.4)$$

$$m_{\alpha_1,\alpha_2} = \frac{1}{\alpha_2 + 1} m_{\alpha_1,0} \quad (5.5)$$

From these general formulas we obtain the means and the standard deviations as

$$\mu_1 = \frac{\lambda_1 - 1}{2\lambda_1(1 - \lambda_2)}, \quad \mu_2 = \frac{1}{2} \quad (5.6)$$

$$\sigma_1 = \left\{ \frac{\lambda_1^2 - 1}{12\lambda_1^2(1 - \lambda_2^2)} \right\}^{1/2}, \quad \sigma_2 = \left\{ \frac{1}{12} \right\}^{1/2} \quad (5.7)$$

The central moments $\bar{m}_{\alpha_1,\alpha_2}$ are given by

$$\bar{m}_{\alpha_1,\alpha_2} = \begin{cases} 0 & \text{if } \alpha_2 \text{ is odd} \\ \frac{1}{2^{\alpha_2}(\alpha_2 + 1)} \bar{m}_{\alpha_1,0} & \text{if } \alpha_2 \text{ is even} \end{cases} \quad (5.8)$$

where

$$\bar{m}_{\alpha_1,0} = \sum_{l=0}^{\alpha_1} (-1)^{\alpha_1-l} \binom{\alpha_1}{l} \mu_1^{\alpha_1-l} m_{l,0} \quad (5.9)$$

Next, we turn to the central correlation function matrix $\bar{R}(1)$. We have

$$\begin{aligned} \bar{R}_{11}(1) &= \frac{(\lambda_1^2 - 1)\lambda_2}{12\lambda_1^2(1 - \lambda_2^2)}, & \bar{R}_{12}(1) &= \frac{\lambda_1^2 - 1}{12\lambda_1^2} \\ \bar{R}_{21}(1) &= 0, & \bar{R}_{22}(1) &= \frac{1}{12\lambda_1} \end{aligned} \quad (5.10)$$

Some other analytical expressions for $\bar{R}_{ij}(k)$ for $k > 1$ have also been derived.

Having the exact values for the moments and correlation functions, we can assess the accuracy of the results obtained by using the GCM method as described in Section 3. The results are given in Table I. For the GCM results

Table I. Statistical Data for the Map (5.1) with $\lambda_1 = 3$ and $\lambda_2 = 1/4$

$N_1 = N_2 =$ $N(B_{SA})$	GCM			Exact value	10^6 iterations (with 10^3 preliminary iterations)		
	10	50	100		Initial state: $x_1 = x_2 =$		
	90	1799	6000		0.001	0.2	0.4
μ_1	0.4455	0.4444	0.4445	$4/9 \sim 0.4444$	0.4444	0.4446	0.4440
μ_2	0.5000	0.5000	0.5000	$1/2 = 0.5$	0.4999	0.5002	0.4995
σ_1	0.2767	0.2809	0.2811	$(32/405)^{1/2} \sim 0.2811$	0.2808	0.2812	0.2811
σ_2	0.2872	0.2886	0.2887	$(1/12)^{1/2} \sim 0.2887$	0.2885	0.2889	0.2887
$\bar{m}_{2,0}$	0.0766	0.0789	0.0790	$32/405 \sim 0.0790$	0.0789	0.0791	0.0790
$\bar{m}_{1,1}$	-0.0031	0.0006	-0.0004	0	0.0001	0.0002	0.0000
$\bar{m}_{0,2}$	0.0825	0.0833	0.0833	$1/12 \sim 0.0833$	0.0832	0.0835	0.0833
$\bar{m}_{3,0}$	0.0001	0.0001	0.0000	0	0.0001	-0.0000	0.0000
$\bar{m}_{2,1}$	-0.0001	0.0000	-0.0000	0	0.0000	0.0000	0.0000
$\bar{m}_{1,2}$	0.0000	0.0000	0.0000	0	0.0000	0.0000	0.0001
$\bar{m}_{0,3}$	-0.0000	-0.0000	-0.0000	0	0.0000	-0.0000	0.0001
$\bar{m}_{4,0}$.0096	0.0104	0.0104	$29184/2788425 \sim 0.0105$	0.0103	0.0105	0.0105
$\bar{m}_{3,1}$	-0.0003	0.0001	-0.0000	0	-0.0000	0.0000	0.0000
$\bar{m}_{2,2}$	0.0067	0.0066	0.0066	$8/1215 \sim 0.0066$	0.0065	0.0066	0.0066
$\bar{m}_{1,3}$	-0.0004	0.0002	-0.0001	0	-0.0000	0.0000	0.0000
$\bar{m}_{0,4}$	0.0121	0.0125	0.0125	$1/80 = 0.0125$	0.0124	0.0125	0.0125
$\bar{R}_{11}(1)$	0.0180	0.0201	0.0196	$8/405 \sim 0.0198$	0.0196	0.0200	0.0198
$\bar{R}_{21}(1)$	-0.0056	0.0006	-0.0006	0	-0.0000	0.0001	0.0001
$\bar{R}_{12}(1)$	0.0714	0.0740	0.0740	$2/27 \sim 0.0741$	0.0738	0.0742	0.0741
$\bar{R}_{22}(1)$	0.0255	0.0282	0.0276	$1/36 \sim 0.0278$	0.0277	0.0280	0.0278
$\bar{R}_{11}(2)$	-0.0012	0.0052	0.0042	$2/405 \sim 0.0049$	0.0050	0.0051	0.0050
$\bar{R}_{21}(2)$	0.0008	0.0011	0.0001	0	-0.0002	0.0000	0.0001
$\bar{R}_{12}(2)$	0.0419	0.0434	0.0432	$7/162 \sim 0.0432$	0.0431	0.0434	0.0432
$\bar{R}_{22}(2)$	0.0025	0.0097	0.0085	$3/324 \sim 0.0093$	0.0093	0.0094	0.0093
$\bar{R}_{11}(3)$	0.0002	0.0022	0.0012	$1/810 \sim 0.0012$	0.0011	0.0013	0.0013
$\bar{R}_{21}(3)$	0.0007	0.0006	-0.0001	0	-0.0000	0.0001	0.0000
$\bar{R}_{12}(3)$	0.0126	0.0191	0.0183	$111/5832 \sim 0.0190$	0.0192	0.0192	0.0190
$\bar{R}_{22}(3)$	0.0015	0.0042	0.0030	$9/2916 \sim 0.0031$	0.0029	0.0031	0.0032
CPU time in sec. ^a	7.8	166.3	563.3		4642.7	4386.4	4435.3

^a VAX 11/750 CPU time. VAX 11/750 is a multi-user system. The CPU time is, therefore, dependent upon the number of users during the time of computation.

we show three sets of data; they are, respectively, for $N_1 = N_2 = 10, 50,$ and 100 . The number of samplings taken in each cell is 5×5 in all cases. One sees that the case $N_1 = N_2 = 100$ produces excellent results with deviations no bigger than two units in the fourth decimal place except $\bar{m}_{1,1}, \bar{R}_{11}(2), \bar{R}_{22}(2),$ and $\bar{R}_{12}(3)$. The case $N_1 = N_2 = 50$ produces reasonably good results except $\bar{R}_{ij}(3)$. It is also remarkable that even the very coarse cell structure of $N_1 = N_2 = 10$ produces good results for the lower-order moments and $\bar{R}_{ij}(1)$.

In the table we also show the statistical values evaluated by direct iteration. Here an initial point was first iterated 1000 times, and then the various statistical quantities were computed by using the next 10^6 iterations. The table shows three sets of data of this kind for three different initial points. A comparison between this conventional iteration method and the present GCM method will be made in the next section.

6. SOME COMMENTS ON THE GCM METHOD AND THE ITERATION METHOD

When Table I is examined, one notes that the accuracy of the iteration method using 10^6 iterations is approximately comparable to that of the GCM method using 100×100 cells for the unit square and 5×5 sampling points for each cell. On the other hand, so far as the computation effort is concerned, the GCM method has an advantage of 1 to 8 in CPU time.

While the computation time comparison is interesting, it is perhaps more important to note the basic difference between the two methods. First, consider the iteration method. If we regard an infinitely long mapping trajectory covering the strange attractor as a random process, then the trajectory generated from a specific initial point is merely a sample of finite length of this process. Each initial point generates one of such samples. This is exhibited by the three quite different sets of statistical data generated by three different initial points in Table I. The standard errors of the data are, in general, of the order $N^{-1/2}$, with N being the sample length. To obtain a set of truly meaningful statistical data based upon, say, 10^6 iterations, we should probably take many samples of this length and then take the ensemble averages. This would, of course, require even a greater computational effort.

On the other hand, the GCM method is essentially a spatial averaging process. The error involved is, therefore, of an entirely different kind. It results from two processes of discretization: partitioning of the state space into cells and the further subpartitioning of a cell in order to compute the transition probability matrix. Once the transition probability matrix has been determined, statistical data can be computed to any desired accuracy without undue computational effort. Thus, the error of the GCM method is from discretization rather than due to finite sequential statistical sampling as in

the iteration method. We do not have a complete analysis of the GCM discretization error for the map of (5.1), but the following partial results may give us some insight to the error involved.

Let $\lambda_1 = 3$ and $\lambda_2 = 1/4$. Consider a partitioning of the unit square into $N_1 \times N_2$ cells. Let $S_1 \times S_2$ denotes the number of sampling points taken within each cell for the purpose of computing the transition probability matrix.

(1) For any N_1, N_2 , and S_1 , if S_2 is a multiple of 3, then the persistent group B_{SA} , representing the strange attractor, is consisted of vertical strips with a uniform limiting probability distribution in the x_2 direction along each strip. Therefore,

$$(\mu_2)_{GCM} = 1/2 \tag{6.1}$$

which is also the exact value for μ_2 .

(2) If the unit square is partitioned into $(3 \times 4^n) \times 1$ cells and (3×3) sampling points are taken within each cell, then it is possible to derive analytically the following expression for μ_1 , based upon the GCM method,

$$(\mu_1)_{GCM} = \frac{9 - 8(1 - 4^n)}{18 \times 4^n} \tag{6.2}$$

As $n \rightarrow \infty$, one recovers the exact value

$$(\mu_1)_{exact} = 4/9 \tag{6.3}$$

The error for a specific value of n and with (3×3) sampling is, therefore,

$$\text{error of } (\mu_1)_{GCM} = \frac{1}{18 \times 4^n} \tag{6.4}$$

Taking now $N = 3 \times 4^n \times 3 \times 3$ iterations as the comparable computation required in this case for the direct iteration method, the statistical error $O(N^{-1/2})$ involved will be of the order 2^{-n} . This error is seen to be much worse than the error of the order 4^{-n} for the GCM method.

Considering all the factors, one might perhaps say that the GCM approach is, in a sense, a more direct and robust way of evaluating the statistical properties of strange attractors. We also believe that the method is a more appropriate and fruitful one to use when we wish to study other properties of strange attractors such as Hausdorff dimension, Liapunov exponents, and entropy, etc.

7. HÉNON-POMEAU MAP

As the next problem we examine the Hénon-Pomeau map:

$$\begin{aligned}x_1(n+1) &= 1 + x_2(n) - a[x_1(n)]^2 \\x_2(n+1) &= bx_1(n)\end{aligned}\tag{7.1}$$

Simo⁽²⁰⁾ has given an excellent discussion of the complex behavior of this map for various values of the parameters a and b . We shall study the statistical properties of two particular cases, namely: the case of $a = 1.4$ and $b = 0.3$ and the case of $a = 1.07$ and $b = 0.3$.

7.1. The Case $a = 1.4$ and $b = 0.3$

For this case there is a strange attractor. In Figs. 2 and 3 we show two persistent groups B_{SA} obtained by using GCM method. For Fig. 2, $N_1 = 300$

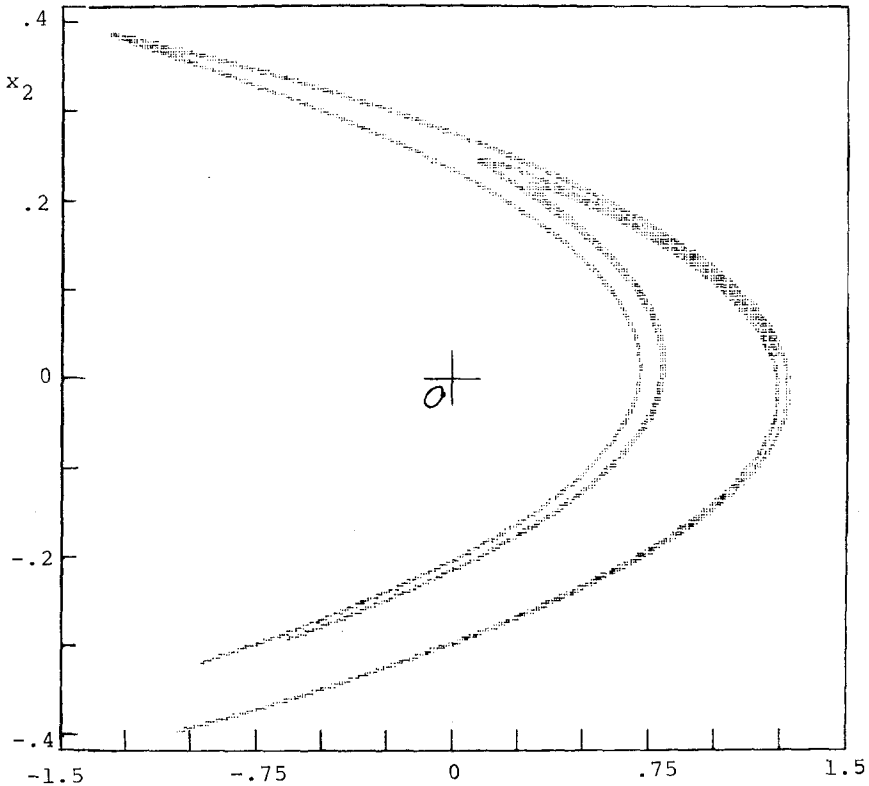


Fig. 2. The persistent group representing the strange attractor of Hénon-Pomeau map for $a = 1.4$ and $b = 0.3$. $N_1 = 300$ covering $-1.5 \leq x_1 \leq 1.5$; $N_2 = 240$ covering $-0.5 \leq x_2 \leq 0.4$.

and $N_2 = 240$ are used to cover $-1.5 \leq x_1 \leq 1.5$ and $-0.4 \leq x_2 \leq 0.4$ while in Fig. 3 $N_1 = 2200$ and $N_2 = 1760$ are used for the same ranges of x_1 and x_2 . Figure 4 is a magnified small region of Fig. 3 covering $0.6 \leq x_1 \leq 0.9$ and $0.1 \leq x_2 \leq 0.2$; it demonstrates the capability of the GCM method to disclose the finer structure of the attractor.

Having located the persistent group, we can compute the limiting probability distribution and various statistical quantities. They are given in Table II. Since we have no analytical result to compare with, we list here some statistical quantities obtained after 10 millions iterative mapping steps for comparison.

7.2. The Case of $a = 1.07$ and $b = 0.3$

For this case there is a strange attractor which is consisted of four separate pieces.⁽¹⁷⁾ Figure 5 shows the persistent group (period 4) representing the strange attractor when $N_1 = N_2 = 1000$ are used to cover $-1.5 \leq x_1 \leq 1.5$ and $-0.5 \leq x_2 \leq 0.5$. Table III shows certain statistical properties of this persistent group as well as those of the persistent group obtained by using a coarser cell structure $N_1 = N_2 = 500$.

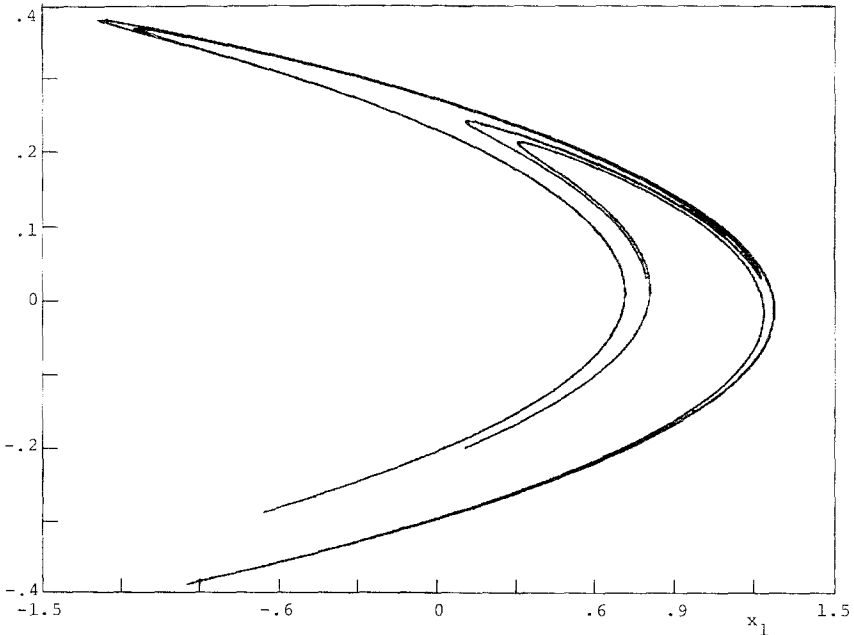


Fig. 3. The persistent group representing the strange attractor of Hénon-Pomeau map for $a = 1.4$ and $b = 0.3$. $N_1 = 2200$ covering $-1.5 \leq x_1 \leq 1.5$; $N_2 = 1760$ covering $-0.4 \leq x_2 \leq 0.4$.

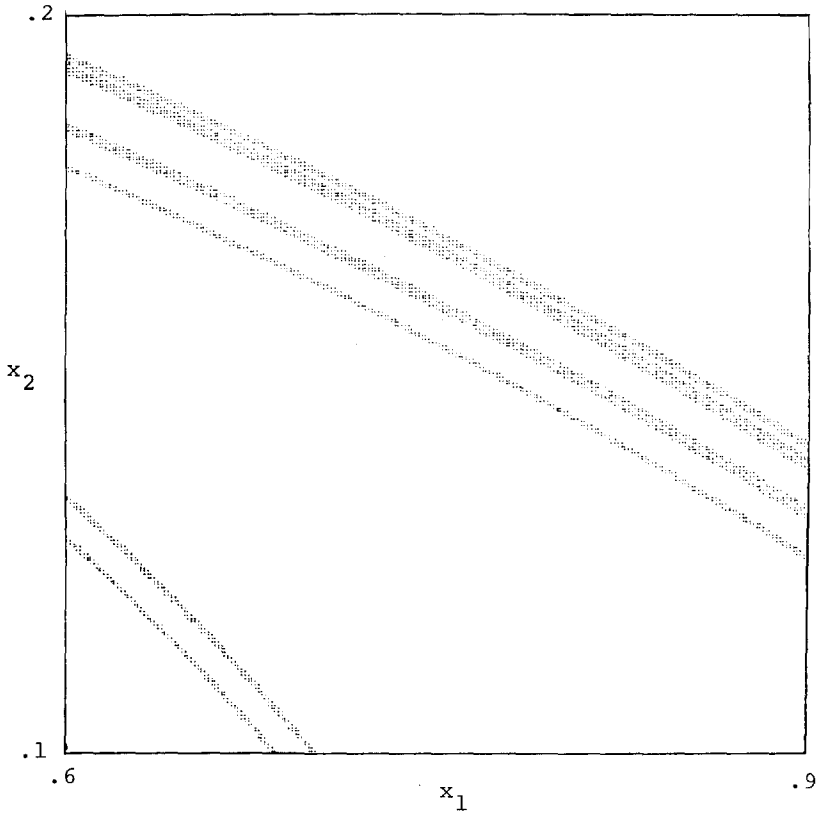


Fig. 4. A magnified portion of Fig. 6. $0.6 \leq x_1 \leq 0.9$; $0.1 \leq x_2 \leq 0.2$.

8. ZASLAVSKII MAP AND A SIMPLE IMPACTED BAR MODEL

Next, we consider the Zaslavskii map^(5,21) which is taken here to be

$$\begin{aligned} x(n+1) &= x(n) + y(n+1) \quad \text{mod } 1 \\ y(n+1) &= \lambda y(n) + k \sin[2x(n)] \end{aligned} \quad (8.1)$$

In physics the mapping has been used to study the motion of charged particles or the Fermi acceleration problem. This map has extremely complex behavior and for certain ranges of values of λ and k it possesses strange attractors.

In engineering a simple mechanical system has been studied.^(22,23) It consists of merely a rigid bar hinged at one end and acted upon at the other end by a periodic impact force of fixed magnitude and direction. The motion

Table II. Statistical Data of a Strange Attractor of Hénon–Pomeau Map with $a = 1.4$ and $b = 0.3$ (GCM: covering $-1.5 \leq x_1 \leq 1.5$, $-0.4 \leq x_2 \leq 0.4$)

$N_1 \times N_1$	GCM				Iteration 10^7
	300×240	300×240	300×240	1500×1200	
Sampling	5×5	9×9	13×13	5×5	
$N(B_{SA})$	2812	3038	3096	19083	
μ_1	0.2557	0.2559	0.2558	0.2566	0.2569
μ_2	0.0767	0.0768	0.0767	0.0770	0.0771
σ_1	0.7219	0.7217	0.7218	0.7212	0.7210
σ_2	0.2166	0.2165	0.2165	0.2164	0.2163
$\bar{m}_{2,0}$	0.5211	0.5209	0.5210	0.5101	0.5199
$\bar{m}_{1,1}$	-0.0520	-0.0520	-0.0521	-0.0500	-0.0488
$\bar{m}_{0,2}$	0.0469	0.0469	0.0469	0.0468	0.0468
$\bar{m}_{3,0}$	-0.1798	-0.1798	-0.1797	-0.1838	-0.1860
$\bar{m}_{2,1}$	0.0317	0.0317	0.0317	0.0314	0.0309
$\bar{m}_{1,2}$	-0.0230	-0.0229	-0.0229	-0.0233	-0.0234
$\bar{m}_{0,3}$	-0.0049	-0.0049	-0.0049	-0.0049	-0.0050
$\bar{m}_{4,0}$	0.5682	0.5680	0.5679	0.5720	0.5735
$\bar{m}_{3,1}$	-0.0751	-0.0751	-0.0752	-0.0749	-0.0744
$\bar{m}_{2,2}$	0.0319	0.0319	0.0319	0.0322	0.0323
$\bar{m}_{1,3}$	-0.0005	-0.0005	-0.0005	-0.0003	-0.0002
$\bar{m}_{0,4}$	0.0046	0.0046	0.0046	0.0046	0.0046
$\bar{R}_{11}(1)$	-0.1734	-0.1735	-0.1737	-0.1662	-0.1628
$\bar{R}_{21}(1)$	0.1563	0.1563	0.1563	0.1560	0.1560
$\bar{R}_{12}(1)$	0.0398	0.0398	0.0398	0.0387	0.0387
$\bar{R}_{22}(1)$	-0.0156	-0.0156	-0.0156	-0.0150	-0.0147
$\bar{R}_{11}(2)$	0.1327	0.1327	0.1328	0.1291	0.1288
$\bar{R}_{21}(2)$	-0.0520	-0.0520	-0.0521	-0.0499	-0.0488
$\bar{R}_{12}(2)$	-0.0610	-0.0610	-0.0611	-0.0606	-0.0600
$\bar{R}_{22}(2)$	0.0119	0.0119	0.0119	0.0116	0.0116
$\bar{R}_{11}(3)$	-0.2035	-0.2034	-0.2036	-0.2022	-0.2004
$\bar{R}_{21}(3)$	0.0398	0.0398	0.0398	0.0387	0.0387
$\bar{R}_{12}(3)$	0.0115	0.0116	0.0117	0.0093	0.0084
$\bar{R}_{22}(3)$	-0.0183	-0.0183	-0.0183	-0.0182	-0.0180

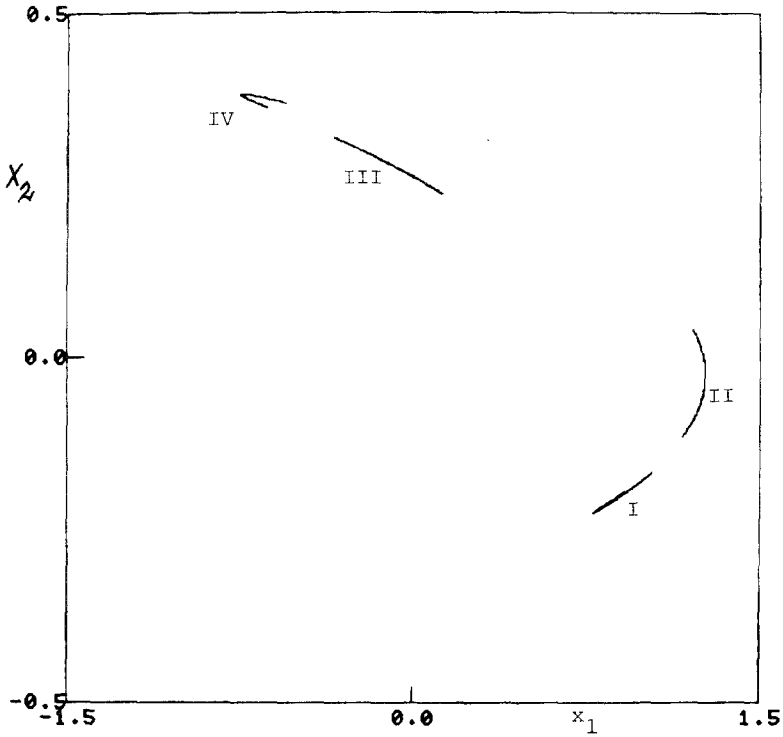


Fig. 5. The persistent group representing the four-piece strange attractor of the Hénon-Pomeau map for $a = 1.07$ and $b = 0.3$. $N_1 = N_2 = 1000$ covering $-1.5 \leq x_1 \leq 1.5$ and $-0.5 \leq x_2 \leq 0.5$.

of the bar may also be resisted by a linear rotational damper at the hinged end. For this simple mechanical system the equation of motion can be integrated exactly over one period of the forcing, leading to the following point mapping

$$\begin{aligned}
 x_1(n+1) &= x_1(n) + \frac{1 - e^{-2\mu}}{2\mu e^{-2\mu}} x_2(n+1) \\
 x_2(n+1) &= -e^{-2\mu} [\alpha \sin x_1(n) - x_2(n)]
 \end{aligned}
 \tag{8.2}$$

where x_1 and x_2 are respectively, the angular displacement and the angular velocity of the rigid bar, μ is a parameter of damping and α is a parameter representing the strength of the impact force.

Table III. Statistical Data on the Four-Piece Strange Attractor of the Hénon–Pomeau Map with $a = 1.07$ and $b = 0.3$

		$N_1 = N_2 = 500$ Sampling 5×5	$N_1 = N_2 = 1000$ Sampling 5×5
Piece I	$N(B_{SA})$	104	206
	μ_1	0.8903	0.8891
	μ_2	-0.2006	-0.2009
	σ_1	0.0824	0.0810
	σ_2	0.0184	0.0181
Piece II	$N(B_{SA})$	127	223
	μ_1	1.2411	1.2435
	μ_2	-0.0180	-0.0156
	σ_1	0.0201	0.0176
	σ_2	0.0435	0.0409
Piece III	$N(B_{SA})$	130	272
	μ_1	-0.0553	-0.0545
	μ_2	0.2679	0.2669
	σ_1	0.1406	0.1397
	σ_2	0.0246	0.0245
Piece IV	$N(B_{SA})$	83	138
	μ_1	-0.6670	-0.6694
	μ_2	0.3723	0.3728
	σ_1	0.0633	0.0607
	σ_2	0.0059	0.0054

While (8.1) and (8.2) are derived separately to treat two different physical problems, they are one and the same mapping. Indeed, if we set

$$\begin{aligned}
 x_1(n) &= 2\pi x(n) - \pi, & x_1(n+1) &= 2\pi x(n+1) - \pi \\
 x_2(n) &= \frac{4\pi\mu e^{-2\mu}}{1 - e^{-2\mu}} y(n), & x_2(n+1) &= \frac{4\pi\mu e^{-2\mu}}{1 - e^{-2\mu}} y(n+1)
 \end{aligned}
 \tag{8.3}$$

we can readily transform (8.2) into (8.1) and vice versa, with the following relations between the two sets of parameters:

$$\begin{aligned}
 \lambda &= e^{-2\mu}, & k &= \frac{1 - e^{-2\mu}}{4\pi\mu} \alpha \\
 \mu &= -\frac{1}{2} \ln \lambda, & \alpha &= \frac{-2\pi k \ln \lambda}{1 - \lambda}
 \end{aligned}
 \tag{8.4}$$

The transformation (8.3) is, of course, formally a trivial matter. However, the identification of (8.1) to a simple mechanical model of (8.2) could perhaps offer a new way of interpreting the complex results of the mapping, a way which is both more elementary and easier to visualize and appreciate.

A fairly extensive study of the statistical properties of strange attractors of the Zaslavskii map has been carried out using the GCM method. Here we shall report three sets of data. For all the results reported below 5×5 sampling points per cell are used. Other choices of sampling points per cell seem to lead to the same results within about 2×10^{-3} as long as there are at least 3×3 sampling points in each cell.

8.1. The Case $\lambda = 0.1$ and $k = 1.4$

Figure 6 shows the persistent group representing the strange attractor obtained by the GCM method using $N_1 = N_2 = 200$ covering $0 \leq x \leq 1$ and

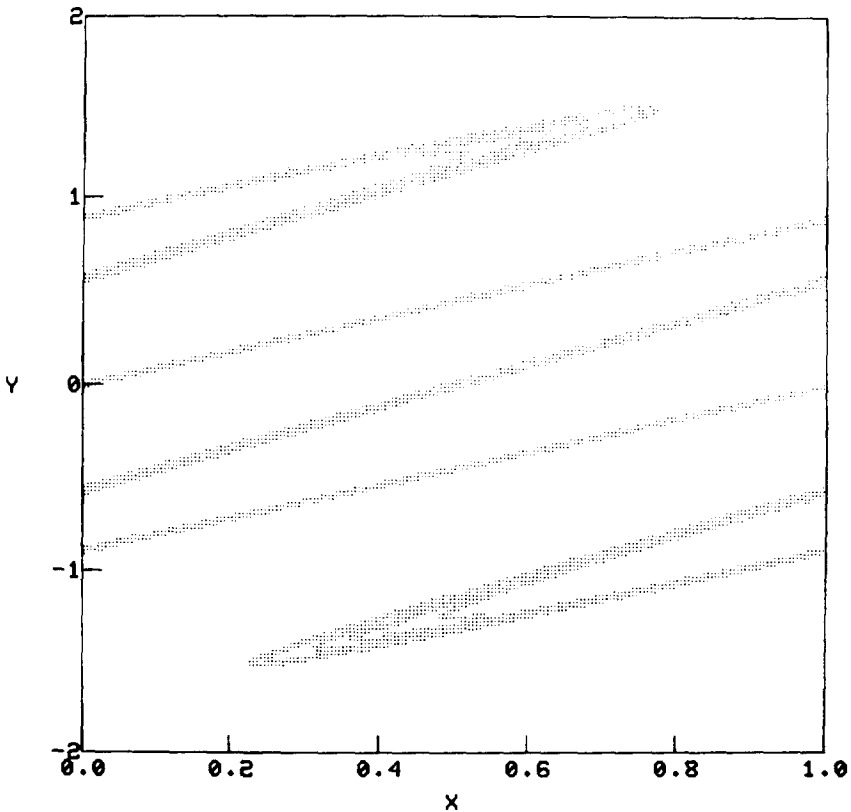


Fig. 6. The persistent group representing the strange attractor of Zaslavskii map for $\lambda = 0.1$ and $k = 1.4$. $N_1 = N_2 = 200$ covering $0 \leq x \leq 1$ and $-2 \leq y \leq 2$.

Table IV. Statistical Data of a Strange Attractor of Zaslavskii Map with $\lambda = 0.1$ and $k = 1.4$ (GCM: Covering $0 \leq x \leq 1, -2 \leq y \leq 2$)

	GCM			10 ⁶ iterations (with 10 ³ preliminary iterations)		
	$N_1 = N_2 =$ $N(B_{SA})$	20 156	100 1208	200 3448	Initial state	
				$x = y =$ 0.001	$x = y =$ 0.2	$x = 0.3,$ $y = 0.5$
μ_1	0.5000	0.5000	0.5000	0.4998	0.4998	0.5004
μ_2	0.0000	0.0000	-0.0000	-0.0000	-0.0000	-0.0020
σ_1	0.2504	0.2465	0.2484	0.2489	0.2488	0.2492
σ_2	0.9677	0.9508	0.9469	0.9486	0.9479	0.9474
$\bar{m}_{2,0}$	0.0627	0.0608	0.0617	0.0619	0.0619	0.0621
$\bar{m}_{1,1}$	0.0069	0.0087	0.0060	0.0058	0.0059	0.0062
$\bar{m}_{0,2}$	0.9365	0.9039	0.8966	0.8998	0.8986	0.8976
$\bar{m}_{3,0}$	-0.0000	-0.0000	-0.0000	-0.0000	-0.0000	-0.0000
$\bar{m}_{2,1}$	-0.0000	-0.0000	0.0000	0.0001	-0.0000	0.0000
$\bar{m}_{1,2}$	-0.0000	-0.0000	-0.0000	0.0003	0.0002	-0.0002
$\bar{m}_{0,3}$	-0.0000	0.0000	0.0000	-0.0001	0.0003	0.0025
$\bar{m}_{4,0}$	0.0087	0.0085	0.0087	0.0087	0.0087	0.0087
$\bar{m}_{3,1}$	-0.0006	-0.0009	-0.0013	-0.0012	-0.0012	-0.0011
$\bar{m}_{2,2}$	0.0382	0.0371	0.0371	0.0372	0.0371	0.0372
$\bar{m}_{1,3}$	0.0438	0.0481	0.0457	0.0437	0.0437	0.0437
$\bar{m}_{0,4}$	1.3969	1.3410	1.3256	1.3306	1.3285	1.3263
$\bar{R}_{11}(1)$	0.0037	0.0022	0.0035	0.0039	0.0038	0.0038
$\bar{R}_{21}(1)$	-0.1919	-0.1857	-0.1853	-0.1870	-0.1869	-0.1870
$\bar{R}_{12}(1)$	0.0316	0.0398	0.0411	0.0408	0.0405	0.0404
$\bar{R}_{22}(1)$	0.0086	-0.0200	-0.0123	-0.0054	-0.0058	-0.0063
$\bar{R}_{11}(2)$	-0.0075	-0.0081	-0.0087	-0.0084	-0.0084	-0.0084
$\bar{R}_{21}(2)$	-0.0262	-0.0163	-0.0203	-0.0226	-0.0222	-0.0222
$\bar{R}_{12}(2)$	-0.0083	-0.0074	-0.0100	-0.0103	-0.0104	-0.0106
$\bar{R}_{22}(2)$	-0.1866	-0.2362	-0.2359	-0.2359	-0.2350	-0.2335
$\bar{R}_{11}(3)$	-0.0009	-0.0006	-0.0001	0.0001	0.0001	0.0001
$\bar{R}_{21}(3)$	0.0401	0.0471	0.0486	0.0480	0.0480	0.0477
$\bar{R}_{12}(3)$	-0.0029	-0.0154	-0.0131	-0.0140	-0.0138	-0.0139
$\bar{R}_{22}(3)$	-0.0059	0.0276	0.0409	0.0402	0.0396	0.0403
CPU time in sec.	73.9	597.7	1715.4	4812.0	4635.2	4723.8

$-2 \leq y \leq 2$. The statistical properties of the persistent groups obtained by using various cell sizes are shown in Table IV. For comparison three sets of results obtained from one million iterative mapping steps are also shown. Considering the fact that μ_1 should have a value $1/2$ and μ_2 and all the third-order central moments should be zero, the results seem to suggest that those from GCM with $N_1 = N_2 = 100$ or 200 might be more reliable than those obtained from 10^6 iterations. It is interesting to see that even the coarse cell structure of $N_1 = N_2 = 20$ leads to very decent results except for the higher-order correlation functions. For this problem we also happened to have the computation time required for various cases and the data are shown at the bottom of Table IV.

8.2. The Case $\lambda = 0.001$

Shown in Fig. 7 are $(m_{0,2}/k^2)$ values vs. k for $\lambda = 0.001$, where $m_{0,2}$ is the second moment with respect to y . The values are computed with the increment of k equal to 0.05 . The data points are linked by straight line

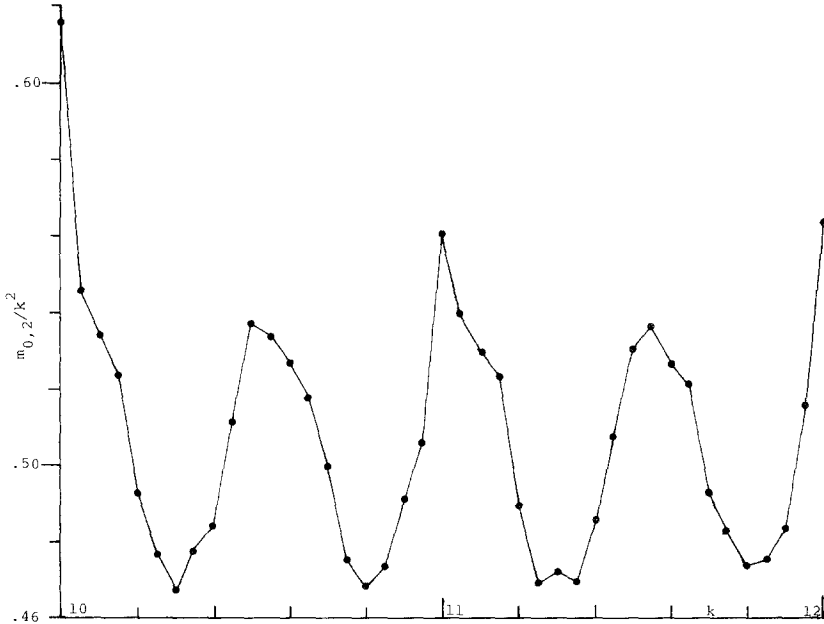


Fig. 7. The value of $m_{0,2}/k^2$ vs. k for the strange attractors of Zaslavskii map with $\lambda = 0.001$. In all cases $N_1 = N_2 = 200$ covering $0 \leq x \leq 1$ and $-15 \leq y \leq 15$, and 5×5 sampling points used in each cell.

segments in order to exhibit the general pattern of the variation. These GCM data may be compared with those shown in Fig. 5 of Ref. 5. In particular, they compare very well with those in Fig. 5 of Ref. 5 designated as iterative mapping results. At $k = 10, 11,$ and 12 the GCM data also exhibit the special character mentioned by Jensen and Oberman.⁽⁵⁾

8.3. Two Cases Where $k < 1$

In most studies of strange attractors of the Zaslavskii map, the value of k is taken to be >1 . In this section we present two cases where $k < 1$. For the discussion of this section we use the mapping (8.2) and use μ and α as the system parameters, instead of λ and k . The statistical data refer to x_1 and x_2 and should be interpreted accordingly.

First consider the case $\mu = 0.3\pi$ and $\alpha = 9$, corresponding to $\lambda = 0.1518$ and $k = 0.6445$. Shown in Fig. 8 is the persistent group representing the

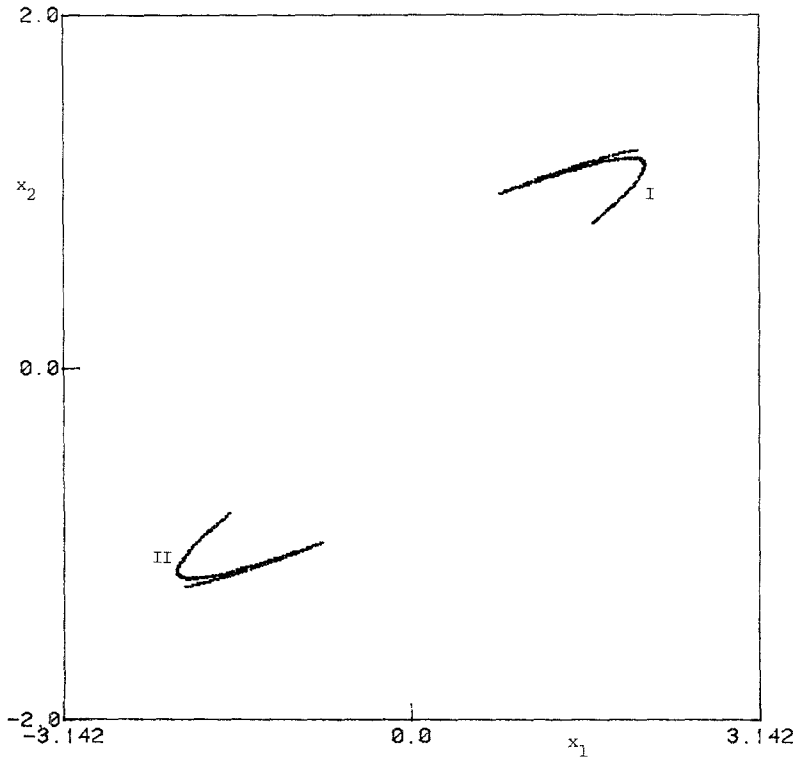


Fig. 8. The persistent group of period 2 representing the two-piece strange attractor of the simple impacted bar model with $\mu = 0.3\pi$ and $\alpha = 9$. $N_1 = N_2 = 500$ covering $-3.142 \leq x_1 \leq 3.142$ and $-2 \leq x_2 \leq 2$.

Table V. Statistical Data of Strange Attractors of the Impacted Bar Model with $\mu = 0.3\pi$ and $\alpha = 9$, and $\mu = 1$ and $\alpha = 9.2$

		$\mu = 1, \alpha = 9.2$					
$\mu = 0.3\pi, \alpha = 9$		Attractor A		Attractor B			
	GCM	Iteration 3×10^5	GCM	Iteration 3×10^5	GCM	Iteration 3×10^5	
	Complete motion		Complete motion		Complete motion		
μ_1	-0.0000	-0.0000	0.3272	0.3263	-0.3272	-0.3263	
μ_2	-0.0000	0.0000	-0.0000	0.0000	0.0000	0.0000	
σ_1	1.6680	1.6685	1.6335	1.6338	1.6335	1.6338	
σ_2	1.0974	1.0970	1.0169	1.0171	0.0169	1.0171	
	Piece I alone		Piece I alone		Piece I alone		
μ_1	1.6204	1.6197	1.9471	1.9463	1.2926	1.2943	
μ_2	1.0936	1.0940	1.0140	1.0143	1.0141	0.0144	
σ_1	0.3973	0.3965	0.1075	0.1078	0.2783	0.2790	
σ_2	0.0916	0.0920	0.0924	0.0926	0.0541	0.0542	

strange attractor obtained by using $N_1 = N_2 = 500$ to cover $-3.142 \leq x_1 \leq 3.142$ and $-2 \leq x_2 \leq 2$. The persistent group is of period 2 representing a strange attractor of two pieces, one in the first quadrant and one in the third. Some statistical data are shown in Table V where the first four data rows are for the complete strange attractor as one motion and the next four

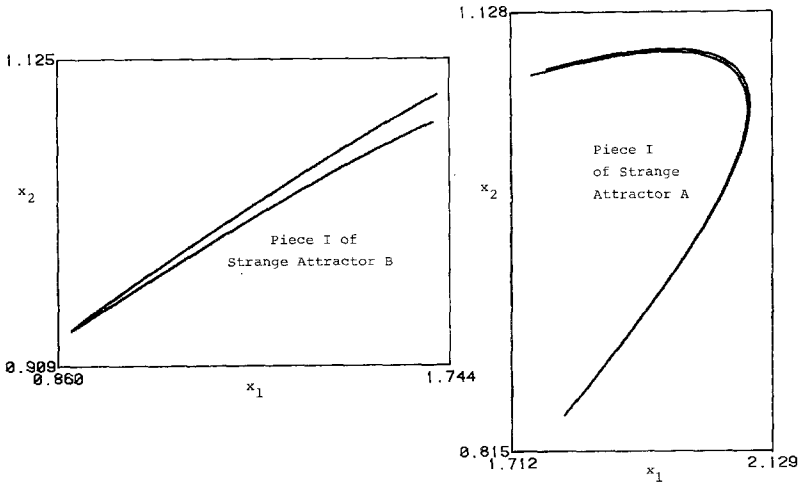


Fig. 9. Persistent subgroups representing Piece I of Strange Attractor A and Piece I of Strange Attractor B for the impacted bar model with $\mu = 1$ and $\alpha = 9.2$.

data rows are for Piece I (one in the first quadrant) taken alone. Of course, Piece I by itself is strange attractor of the system under the G^2 mapping. Also shown for the purpose of comparison are some statistical data obtained by iterative mapping; the agreement is excellent.

Next, we consider the case $\mu = 1$ and $\alpha = 9.2$, corresponding to $\lambda = 0.1353$ and $k = 0.6330$. For this case there are two strange attractors of period 2, to be, respectively, designated as attractor A and attractor B. Again, each is consisted of two pieces, Piece I in the first quadrant and Piece II in the third quadrant. Shown in Fig. 9 are the pieces in the first quadrant. The statistical data for these two attractors are shown in Table V. Some data obtained by iterative mapping are also shown for the purpose of comparison; the agreement is again excellent.

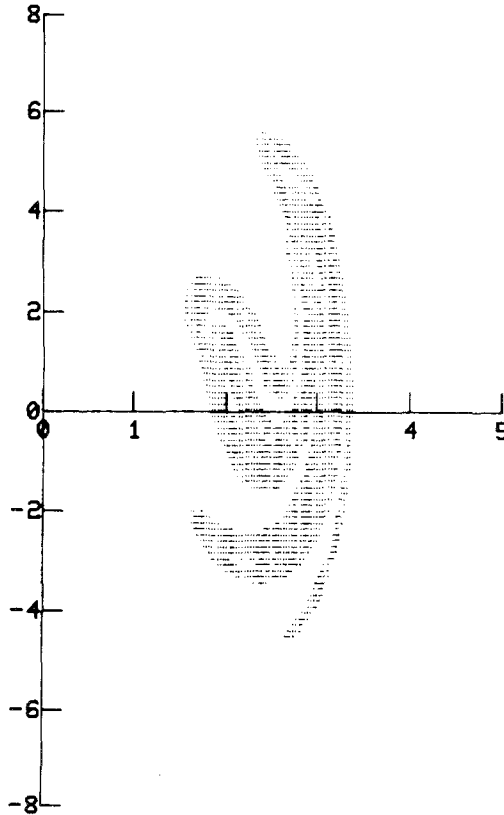


Fig. 10. The persistent group representing the strange attractor of the forced Duffing system (9.1) with $k = 0.05$ and $B = 7.5$. $N_1 = N_2 = 100$ covering $1 \leq x \leq 4$ and $-6 \leq dx/dt \leq 6$.

9. A DUFFING SYSTEM UNDER PERIODIC FORCING

As the last application we consider the strange attractors of systems governed by differential equations. Here we examine a class of Duffing systems under periodic forcing⁽²⁴⁾ governed by

$$\frac{d^2x}{dt^2} + k \frac{dx}{dt} + x^3 = B \cos t \quad (9.1)$$

The strange attractors of such a differential system can again be studied by using the GCM method as described in Section 3 after a cellularly structured phase plane has been introduced. The only difference lies in the way by which the image cells of a cell are computed. With point mappings it is a simple matter to compute the image cell of each sampling point. For systems governed by differential equations we need, however, to integrate numerically the equation over one period, here 2π , in order to obtain the image cell.

Shown in Fig. 10 is the strange attractor for the case $k = 0.05$ and $B = 7.5$. Here $N_1 = N_2 = 100$ are used to cover $1 \leq x \leq 4$ and $-6 \leq dx/dt \leq 6$ and 5×5 sampling points are used in each cell. This GCM result may be compared with Fig. 3 of Ref. 24. The GCM mean values and the standard deviations of this strange attractor, considered only at discrete time $2n\pi$, are shown in Table VI where they are compared against some data obtained from numerically integrating the equation over 10^4 and 10^5 periods.

10. CONCLUDING REMARKS

In this paper we have presented an alternative way to study the strange attractors by using the cell-to-cell mapping concept and Markov chain techniques. It is a simple and yet effective method. The statistical data obtained by this method seem to be quite reliable. Hopefully, the method

Table VI. Statistical Data of the Strange Attractor of the Forced Duffing System with $k = 0.05$ and $B = 7.5$

	GCM	Numerically Integrating over	
		10^4 periods	10^5 periods
μ_1	2.5777	2.5732	2.5755
μ_2	0.3266	0.3150	0.3155
σ_1	0.4694	0.4696	0.4684
σ_2	2.1777	2.1807	2.1664

might also offer us a more attractive approach to follow other than the direct iterative procedure, when we wish to evaluate numerically other properties of strange attractors such as the Hausdorff dimension, Liapunov exponents and entropy.

ACKNOWLEDGMENTS

This material is based upon work supported by the National Science Foundation under grant No. MEA-8217471. The authors also wish to thank two referees for their many helpful comments.

REFERENCES

1. A. J. Lichtenberg and M. A. Lieberman, *Regular and Stochastic Motion* (Springer, New York, 1982).
2. J. Guckenheimer and P. Holmes, *Nonlinear Oscillations, Dynamical Systems and Bifurcations of Vector Fields* (Springer, New York, 1983).
3. M. J. Feigenbaum, *Los Alamo Sci.* 1:4 (1980).
4. E. Ott, *Rev. Mod. Phys.* 53:655 (1981).
5. R. V. Jensen and C. R. Oberman, *Physica* 4D:183 (1982).
6. C. S. Hsu, *J. Appl. Mech.* 47:931 (1980).
7. C. S. Hsu and R. S. Guttalu, *J. Appl. Mech.* 47:940 (1980).
8. C. S. Hsu, *J. Appl. Mech.* 48:634 (1981).
9. C. S. Hsu, R. S. Guttalu, and W. H. Zhu, *J. Appl. Mech.* 49:885 (1982).
10. C. S. Hsu, *J. Appl. Mech.* 49:895 (1982).
11. C. S. Hsu and W. H. Leung, *J. Math. Analysis Applic.* 100:250 (1984).
12. C. S. Hsu, *Int. J. Non-Linear Mechanics* 18:199 (1983).
13. K. L. Chung, *Markov Chains with Stationary Transition Probabilities*, 2nd ed. (Springer, New York, 1967).
14. D. L. Isaacs and R. W. Madsen, *Markov Chains: Theory and Applications* (Wiley, New York, 1976).
15. V. I. Romanovsky, *Discrete Markov Chains* (Wolters-Noordhoff Publishing, Groningen, The Netherlands, 1970).
16. A. N. Kolmogorov and V. M. Tihomirov, *Usp. Mat. Nauk* 14:3 (1959); *Am. Math. Soc. Transl.* 17(2):277 (1961).
17. Ya. Sinai, *Dokl. Akad. Nauk SSSR* 125:1200 (1959).
18. R. Bowen, *Am. J. Math.* 92:725 (1970).
19. R. Shaw, *Z. Naturforsch.* 36a:80 (1981).
20. C. Simo, *J. Stat. Phys.* 21:465 (1979).
21. G. M. Zaslavskii and B. V. Chirikov, *Usp. Fiz. Nauk* 105:3 (1971).
22. C. S. Hsu, H. C. Yee, and W. H. Cheng, *J. Sound Vib.* 50:95 (1977).
23. C. S. Hsu, *Adv. Appl. Mech.* 17:245 (1977).
24. Y. Ueda, *New Approaches to Nonlinear Problems in Dynamics*, P. Holmes, ed. (SIAM, Philadelphia, 1980), p. 311.